

Defective Graphene Aerogel Supported Bi-CoP nanoparticles as High-Potential Air-Cathode for Rechargeable Zn–Air Batteries

Jianping Chen,^a Bangqing Ni,^a Jiugang Hu,^{*c} Zexing Wu,^{*d} Wei Jin,^{*a,b}

^aSchool of Chemical and Material Engineering, Jiangnan University, Wuxi 214122, China

^b Physikalische Chemie, TU Dresden, Bergstraße 66b, 01069 Dresden, Germany

^c College of Chemistry and Chemical Engineering, Central South University, No. 932th South Lushan Road, Changsha, Hunan 410083, China

^d College of Chemistry and Molecular Engineering, Qingdao University of Science & Technology, Qingdao 266042, PR China

**Corresponding author: E-mail: hugiugang@csu.edu.cn (Jiugang Hu);*

splswzx@qust.edu.cn (Zexing Wu); wjin@ipe.ac.cn (Wei Jin).

Part I: Materials and Methods

Reagents and materials

Analytical-grade cobaltous nitrate hexahydrate ($\text{Co}(\text{NO}_3)_2 \cdot 6\text{H}_2\text{O}$), urea ($\text{CH}_4\text{N}_2\text{O}$), phosphoric acid (H_3PO_4), sodium hypophosphite ($\text{NaH}_2\text{PO}_2 \cdot \text{H}_2\text{O}$) were purchased from Sinopharm (Shanghai, China). Graphene oxide was obtained from Nanjing XFNANO (Nanjing, China). $\text{Bi}(\text{NO}_3)_3 \cdot 5\text{H}_2\text{O}$ and commercial RuO_2 were purchased from Shanghai Aladdin Biochemical Technology Co., Ltd (Shanghai, China). Standard Pt/C and 5% Nafion were purchased from Shanghai Macklin Biochemical Co., Ltd (Shanghai, China) and Alfa Aesar (China) Chemical Co., Ltd., respectively.

Synthesis of DGO

Typically, the defects-rich graphene oxide was obtained by acidification. 0.2 g GO was impregnated with 0.5 M H_3PO_4 solution for 24 h. After washed by water and dried at 60 °C under vacuum, the defective graphene oxide (DGO) was received.

Synthesis of Bi-CoP/NP-DG nanocomposite

In a typical procedure, 9.7 mg $\text{Bi}(\text{NO}_3)_3 \cdot 5\text{H}_2\text{O}$ and 29.1 mg $\text{Co}(\text{NO}_3)_2 \cdot 6\text{H}_2\text{O}$ were firstly mixed with a 10 mL aqueous solution containing 1 g urea, and the mixture was continuously stirred to form a homogeneous solution. Then, 5 mL GO solution (8 mg mL^{-1}) was added into the above dispersion and further stirred for another 60 min. Afterwards, the mixture was put into a 25 mL Teflon-lined autoclave, following by hydrothermal treatment at 160 °C for 12 h. Once cooled down to room temperature, the obtained hydrogel was washed with deionized water several times and then via a freeze-drying method (24 h) to yield the aerogel precursor. Subsequently, the obtained aerogel precursor was firstly transferred into a muffle furnace and heated at 350 °C for 30 min in air to synthesize the intermediate. Then, the product intermediate and 1.5 g $\text{NaH}_2\text{PO}_2 \cdot \text{H}_2\text{O}$ were placed in the central and upstream positions of a tube furnace, respectively. After flushed with Ar, the center of the tube furnace was elevated to 400 °C with a ramping rate of 2 °C min^{-1} and held at this temperature for 180 min, and then naturally cooled to ambient temperature under Ar to yield the the nitrogen, phosphorus co-doped defective graphene aerogels supported bismuth-cobalt phosphide particles (Bi-CoP/NP-DG). For comparison, Bi-CoP/NP-G, CoP/NP-G and

pure Bi-CoP composites were also prepared with the similar experimental conditions.

Physicochemical characterization

The surface morphology and structure were determined with field-emission scanning electron microscopy (FE-SEM, JSM-7610F) and high-resolution transmission electron microscopy (HR-TEM, JEOL JEM-2100F). The crystalline phase and elemental states were identified using XRD (X’Pert Pro MPD, Panalytical Company, Cu-K α X-ray) and X-ray photoelectron spectroscopy (XPS, VG ESCALAB MKII, Mg Ka X-ray). Raman spectrum was performed by Horiba Jobin Yvon LabRAM HR800. The electron spin resonance (ESR) analysis were obtained on a JEOL spectrometer (JES-FA200) at ambient temperature. The Brunauer–Emmett–Teller (BET) specific surface area was recorded at 77 K with a Micromeritics ASAP 2050 system.

Electrochemical Measurements

A CHI 760E electrochemical workstation was used with the typical three-electrode system including a rotating disk electrode (RDE, 0.196 cm²), a platinum sheet auxiliary electrode, and a Ag/AgCl reference electrode. The electro-catalyst ink was formed by ultrasonically dispersing 5 mg nanocatalyst, 0.5 mL ethanol, 0.5 mL deionized water and 20 μ L of 5 wt.% Nafion solution. 10 μ L of the as-prepared catalyst ink was pipetted and spread onto the substrate to achieve 250 μ g cm⁻² loading. The ORR tests were performed in O₂-saturated and N₂-purged 0.1 M KOH solution using 5 mV s⁻¹ scan rate and different rotating speed (400-2025 rpm). For the OER, the polarization curves were also measured in 0.1 M KOH solution with 5 mV s⁻¹ scan rate. It should be noted that high-purity O₂ was purged through the solution, and a rotation speed of 1600 rpm was maintained during the OER. The impedance was recorded by electrochemical impedance spectroscopy tests ranging from 0.1 Hz to 100 kHz at open circuit potential with a 5 mV amplitude of sinusoidal potential perturbation.

The Zn-air battery evaluation were performed at a self-made Zn-air cell, in which the air cathode consisted of the loaded hydrophilic carbon paper of 10 mg cm⁻². A polished 0.3 mm thickness Zn plate was used as the anode, while a 0.2 M

$\text{Zn}(\text{CH}_3\text{COO})_2 + 6 \text{ M KOH}$ mixed solution was employed as the electrolyte. The 1 cm^2 gas diffusion layer provides O_2 from ambient air towards the catalyst sites, and a Land CT2001A system was selected to carry out the Zn-air battery tests. Each discharge-charge period were set as 20 min with 10 mA cm^{-2} current density. Based on the discharge curves at a constant current density of 5 mA cm^{-2} , we can calculate the corresponding specific capacity ($\text{mAh g}_{\text{Zn}}^{-1}$) and energy density ($\text{Wh kg}_{\text{Zn}}^{-1}$) by the following equations, respectively.

$$\text{Specific capacity} = \frac{\text{current} \times \text{service hours}}{\text{weight of consumed Zn}}$$

$$\text{Energy density} = \frac{\text{current} \times \text{service hours} \times \text{average discharge voltage}}{\text{weight of consumed Zn}}$$

The overall water splitting was tested in the two-electrode scheme in 1 M KOH. The Bi-CoP/NP-DG was dropped onto a Ni foam substrate in both the anode and cathode. The catalyst loading is 5 mg cm^{-2} .

Part II: Figures and Tables

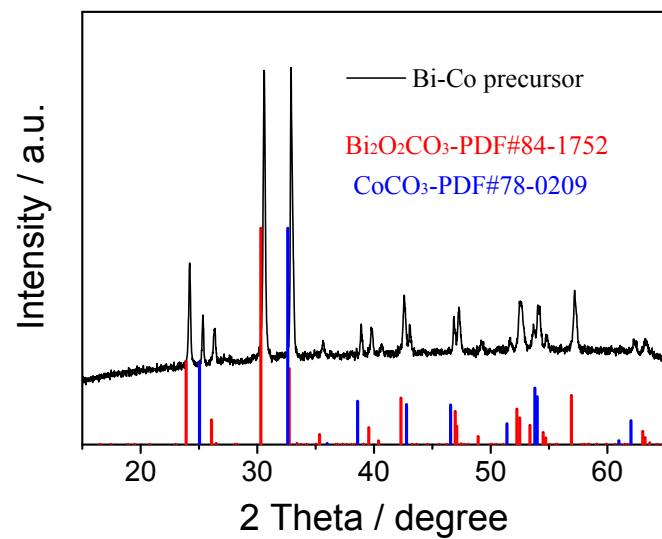


Figure S1. XRD of Bi-Co precursor.

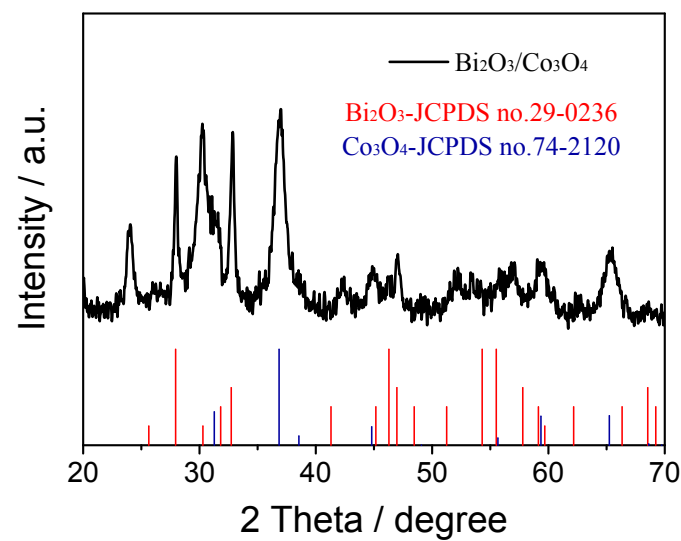


Figure S2. XRD of Bi-Co oxides.

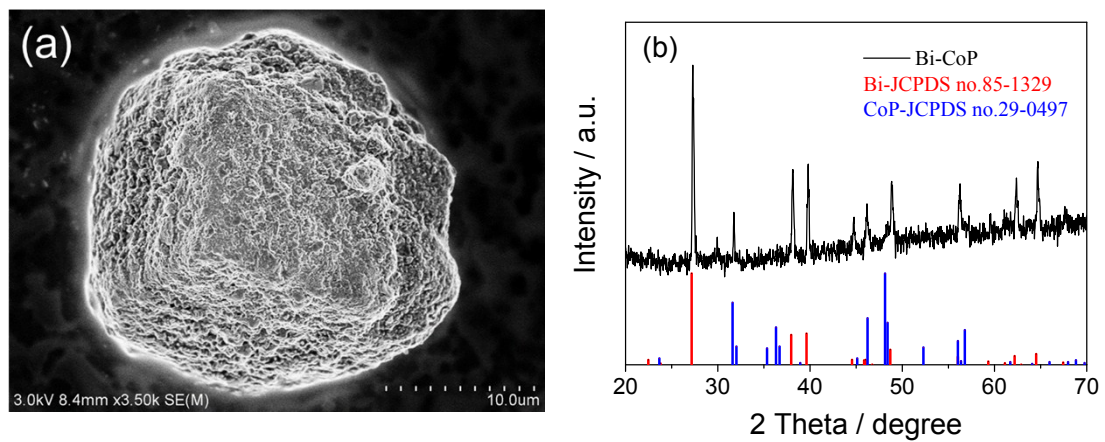


Figure S3. (a) SEM image and (b) XRD of Bi-CoP.

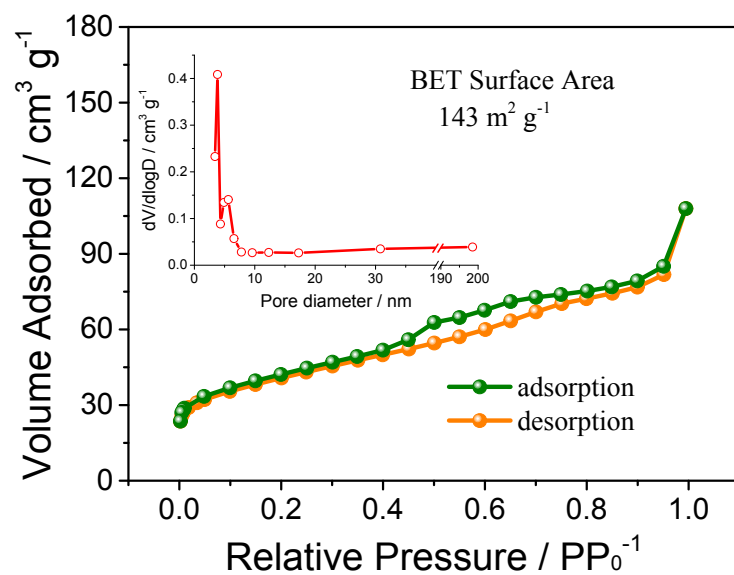


Figure S4. N_2 adsorption-desorption isotherms of the Bi-CoP/NP-DG nanocomposite.

The inset shows the corresponding pore distribution curve.

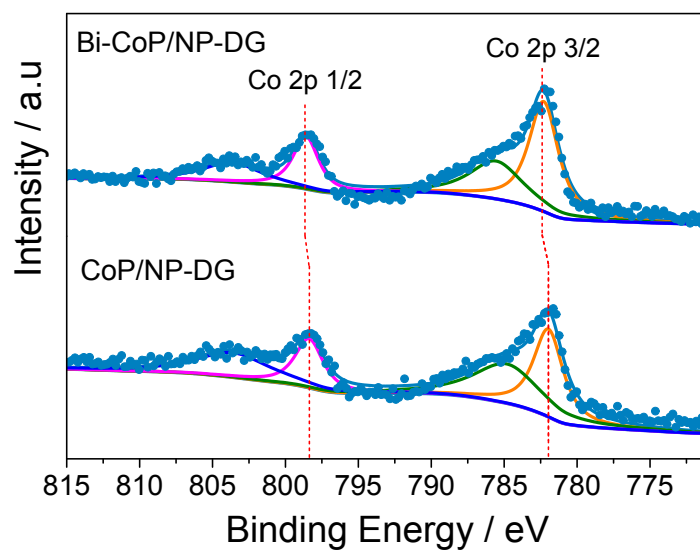


Figure S5. High-resolution XPS spectra of Co 2p core levels in Bi-CoP/NP-DG and CoP/NP-DG.

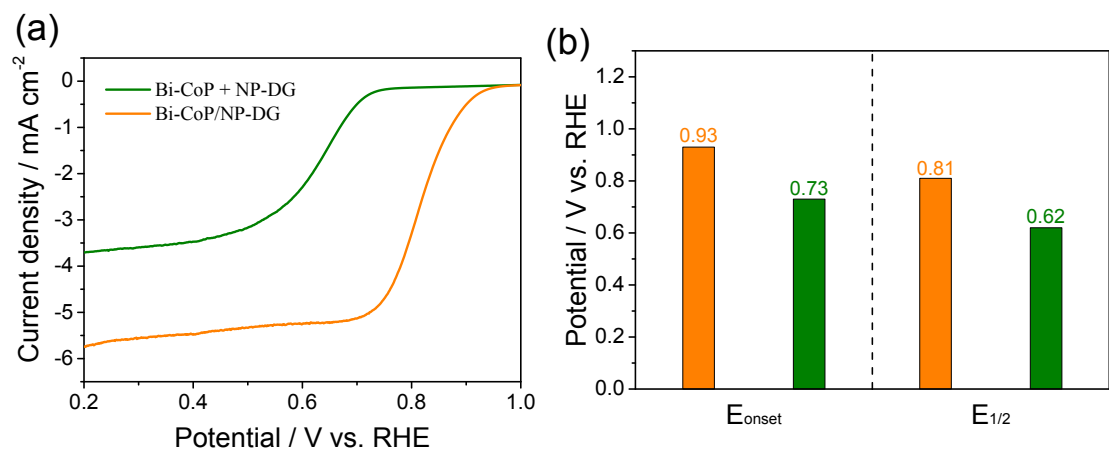


Figure S6. a) ORR polarization curves in O₂-saturated 0.1 M KOH (Rotation rate: 1600 rpm; Sweep rate: 5 mV s⁻¹) of Bi-CoP/NP-DG and Bi-CoP+NP-DG catalysts; b) Bar plots of the E_{onset} and E_{1/2}.

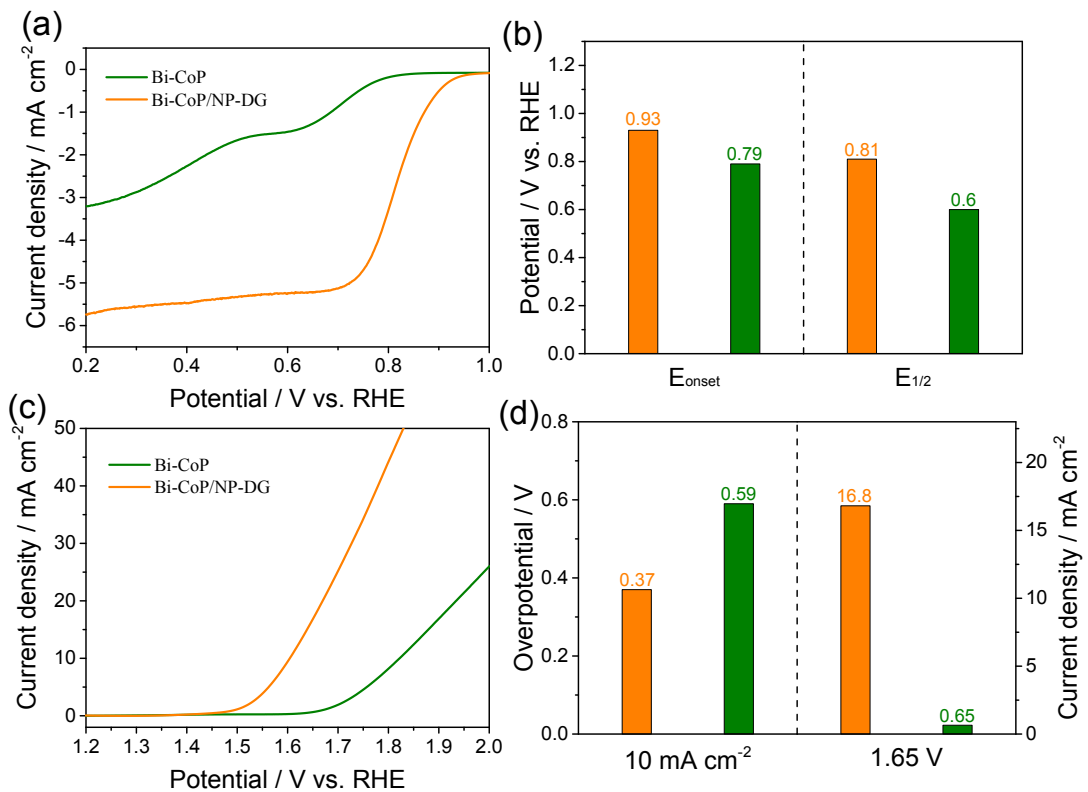


Figure S7. a) ORR polarization curves in O_2 -saturated 0.1 M KOH (Rotation rate: 1600 rpm; Sweep rate: 5 mV s^{-1}) of Bi-CoP/NP-DG and Bi-CoP catalysts; b) Bar plots of the E_{onset} and $E_{1/2}$; c) OER polarization curves in O_2 -saturated 0.1 M KOH (Rotation rate: 1600 rpm; Sweep rate: 5 mV s^{-1}) of Bi-CoP/NP-DG and Bi-CoP catalysts; d) Overpotentials at a chosen current density of 10 mA cm^{-1} and the current densities at a chosen potential of 1.65 V.

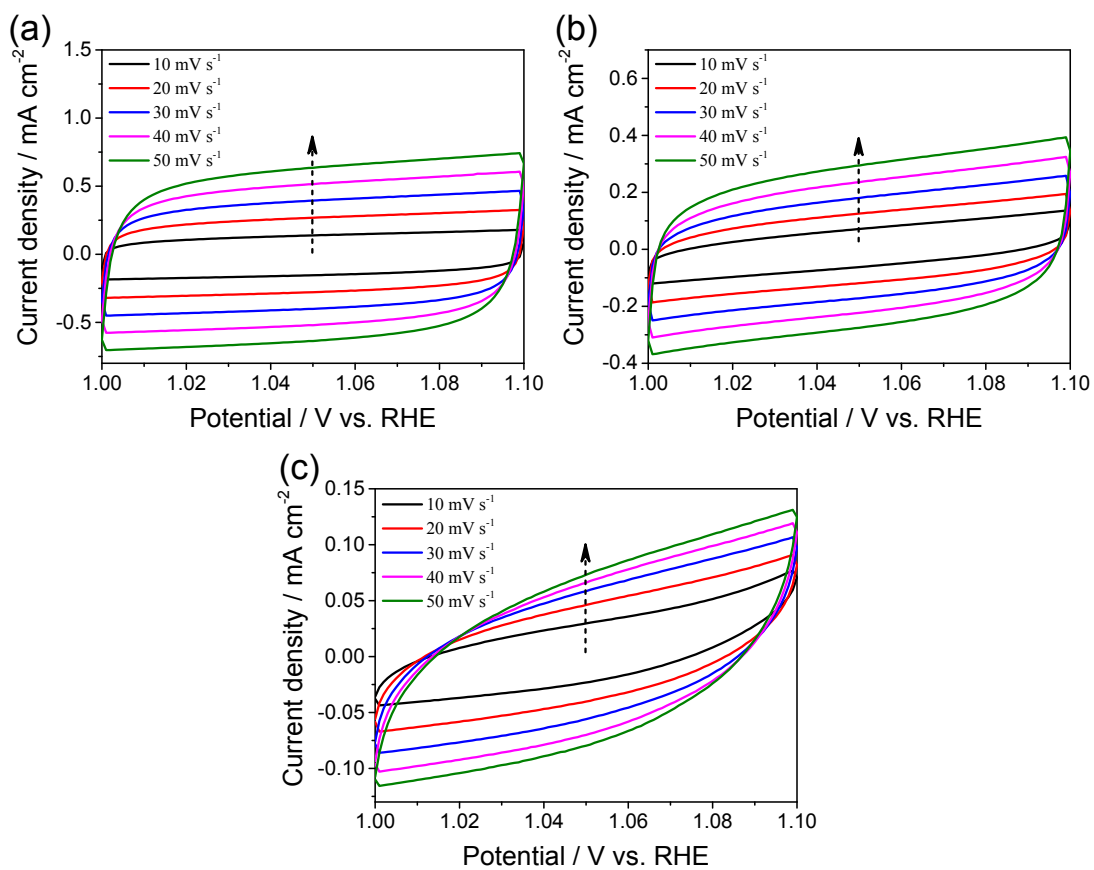


Figure S8. The cyclic voltammograms (CVs) curves at different scan rates of a) Bi-CoP/NP-DG, b) Bi-CoP/NP-G and c) CoP/NP-G.

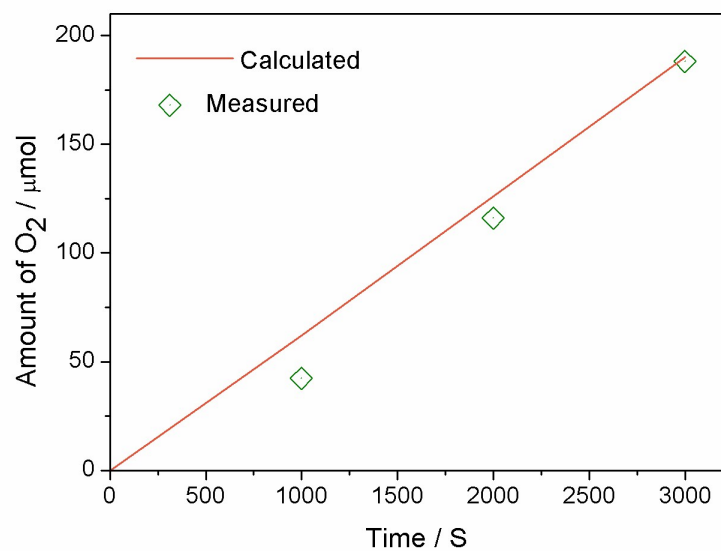


Figure S9. The amount of evolved oxygen gas measured by Bi-CoP/NP-DG during

3000 s.

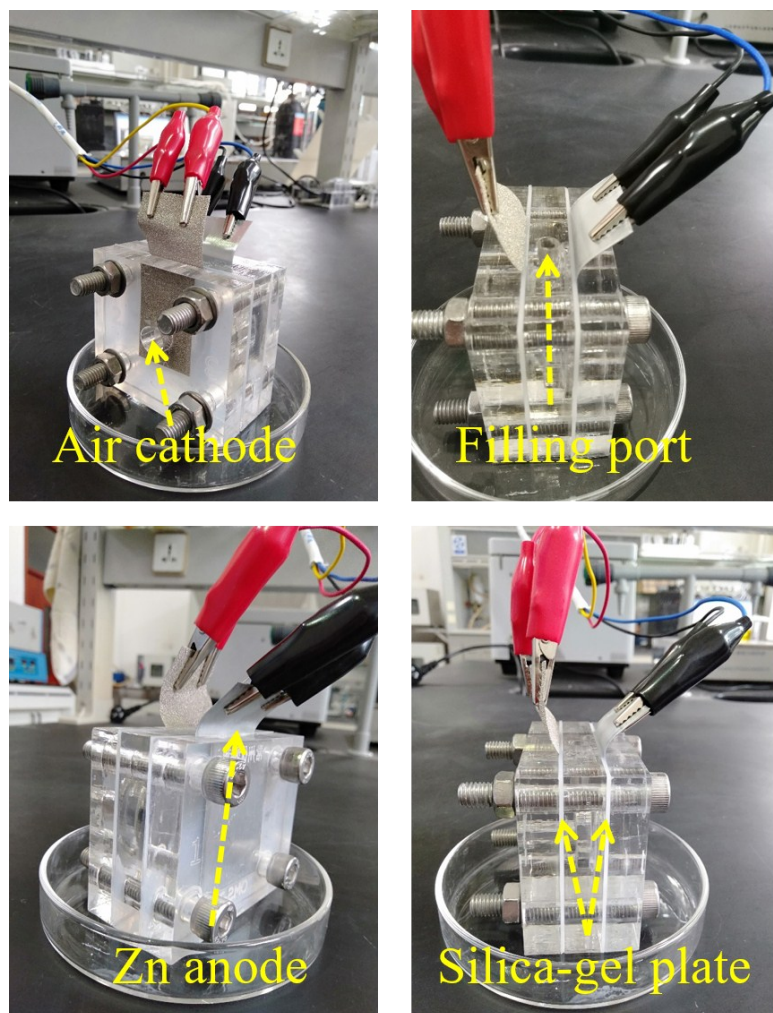


Figure S10. Digital images of the rechargeable Zn-air battery recorded from the different directions.

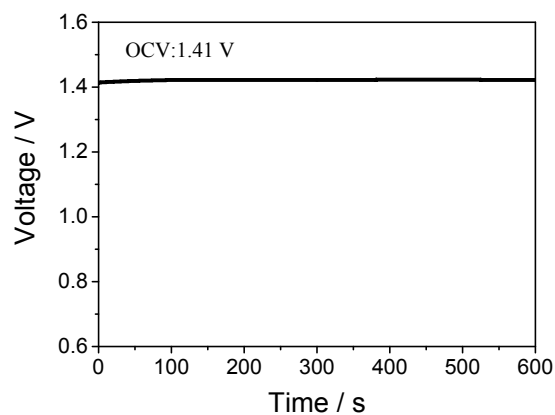


Figure S11. Open-circuit plots of Zn-air battery driven by Bi-CoP/NP-DG.

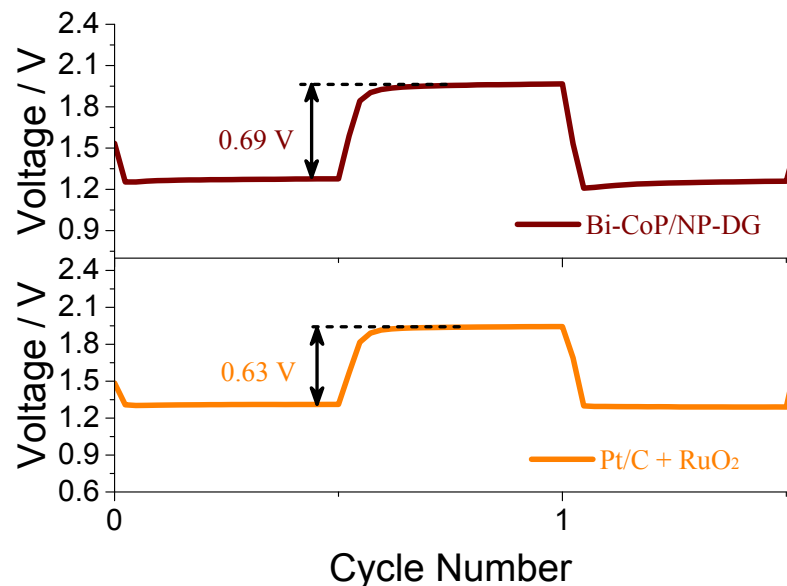


Figure S12. The enlarged 1st cycle discharge and charge voltage profile of Zn-air cells.

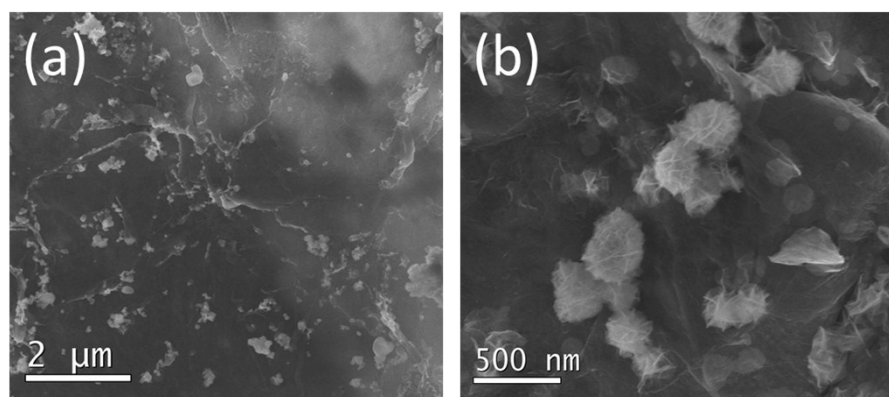


Figure S13. a, b) SEM images of Bi-CoP/NP-DG after the charge/discharge cycles.

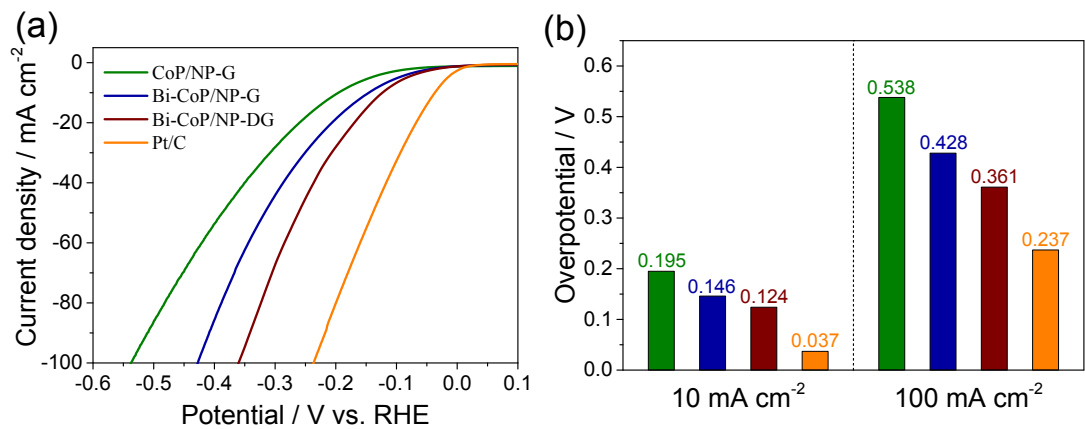


Figure S14. a) HER polarization curves in N_2 -saturated 1 M KOH (Rotation rate: 1600 rpm; Sweep rate: 5 mV s⁻¹) of CoP/NP-G, Bi-CoP/NP-G, Bi-CoP/NP-DG and commercial Pt/C catalysts; b) Overpotentials at a chosen current density of 10 and 100 mA cm^{-1} .

Table S1. Performances of recently reported ORR electrocatalysts. Herein, the

comparison of ORR activity of Bi-CoP/NP-DG with previously reported cobalt based materials and other non-noble metal electrocatalysts were made.

Number	Catalyst	$E_{1/2}$ / V	Electrolyte	Loadings (mg cm ⁻²)	Ref
1	Bi-CoP/NP-DG	0.81	0.1 M KOH	0.25	This work
2	FeCo@NC-750	0.80	0.1 M KOH	0.80	¹
3	Co _{0.5} Fe _{0.5} S@N-MC	0.808	0.1 M KOH	0.80	²
4	Co ₃ O ₄ /N-rGO	0.79	0.1 M KOH	0.128	³
5	CoS _x @PCN/rGO	0.78	0.1 M KOH	0.40	⁴
6	Co/CoO _x	0.76	0.1 M KOH	0.51	⁵
7	Co _{1-x} S/Graphene	0.755	0.1 M KOH	0.10	⁶
8	Co ₃ InC _{0.75} @CN _x	0.75	0.1 M KOH	0.20	⁷
9	Co/N-C-800	0.74	0.1 M KOH	0.25	⁸
10	NiCo ₂ S ₄ -rGO	0.733	0.1 M KOH	0.32	⁹
11	Co ₃ FeS _{1.5} (OH) ₆	0.721	0.1 M KOH	0.255	¹⁰
12	NiCo ₂ S ₄ @N/S-rGO	0.72	0.1 M KOH	0.283	¹¹
13	CuCo ₂ S ₄ NSS	0.7	0.1 M KOH	0.20	¹²
14	NiCo ₂ S ₄ SMS	0.7	0.1 M KOH	0.704	¹³
15	NiO/CoN PINWs	0.68	0.1 M KOH	0.20	¹⁴

Table S2. Comparison of OER activity of Bi-CoP/NP-DG with other OER catalysts

reported before.

Number	Catalyst	Overpotential / V		Loadings (mg cm ⁻²)	Ref
		(10 mA cm ⁻²)	Electrolyte		
1	Bi-CoP/NP-DG	0.37	0.1 M KOH	0.25	This work
2	Co/CoO@Co-N-C	0.38	0.1 M KOH	0.40	15
3	CoZn-NC-700	0.39	0.1 M KOH	0.24	16
4	FeN _x -PNC	0.40	0.1 M KOH	0.14	17
5	NC@Co-NGC DSNC	0.41	0.1 M KOH	0.40	18
6	N-graphene/CNT	0.42	0.1 M KOH	0.20	19
7	Co-N _x B-CSs	0.43	0.1 M KOH	0.10	20
8	NDGs-800	0.45	1 M KOH	0.20	21
9	1100-CNS	0.46	0.1 M KOH	0.42	22
10	Fe@N-C	0.48	0.1 M KOH	0.31	23
11	N-GCNT/FeCo-3	0.50	0.1 M KOH	0.20	24
12	MnO@Co-N/C	0.53	0.1 M KOH	0.13	25
13	NiCo@N-C	0.53	0.1 M KOH	0.40	26
14	N-CN9	0.54	0.1 M KOH	0.21	27
15	NCNF-1000	0.61	0.1 M KOH	0.10	28

Table S3. Comparison of ORR stability of Bi-CoP/NP-DG with other ORR catalysts

reported before.

Number	Catalyst	Electrolyte	Degradation	Time / h	Ref
			ratio / %		
1	Bi-CoP/NP-DG	0.1 M KOH	13	10	This work
2	3D-CNTA	0.1 M KOH	11.5	11.1	5
3	GO-Zn/Co(1:1)-800	0.1 M NaOH	20	2	29
4	Co-NC	0.1 M KOH	22	10	30
5	0.5-Co ₉ S ₈ @N-C	0.1 M KOH	15	5.6	31
6	CoNim	0.1 M KOH	16.7	29	32
7	Co ₃ O ₄ NS/ZTC	0.1 M KOH	15	8.3	33
8	NCN-1000-5	0.1 M KOH	14.4	3.3	34
9	Pd ₃ Co	0.1 M KOH	21	4.2	12
10	Ni ₃ Fe/C	0.1 M KOH	16	3.3	35
11	Au-NWs/Ni ₆ MnO ₈	0.1 M KOH	18	8.3	36
12	MnCo ₂ O ₄ /C	0.1 M KOH	27.5	2.8	37
13	1100-CNS	0.1 M KOH	15	24	38
14	FeZ-CNS	0.1 M HClO ₄	26.7	4.2	39
15	MnO@Co-N/C	0.1 M KOH	14	2	40

Table S4. Comparison of OER stability of Bi-CoP/NP-DG with other OER catalysts

reported before.

Number	Catalyst	Electrolyte	Degradation	Time / h	Ref
			ratio / %		
1	Bi-CoP/NP-DG	0.1 M KOH	36	10	This work
2	Au-NWs/Ni ₆ MnO ₈	0.1 M KOH	39	8.3	³⁶
3	CoFe ₂ O ₄ NPs	1 M KOH	34.7	10	⁴¹
4	Ni ₃ Fe/N-C	0.1 M KOH	49.7	3.3	³⁵
5	CoIn ₂ S ₄ /S-rGO	0.1 M KOH	39.6	1.4	⁴²
6	N-C	0.1 M KOH	35.9	7	²⁶
7	CoO	1 M KOH	38	2.2	⁴³
8	Ni ₃ FeN	0.1 M KOH	40	3.3	⁴⁴
9	Co ₃ O ₄	1 M KOH	55.5	24	⁴⁵
10	Co ₉ S ₈ /rGO	0.1 M KOH	43	11.1	⁴⁶
11	NiIn ₂ S ₄ /CNFs	0.1 M KOH	39.4	1.4	⁴⁷
12	FeCo/N-DNC	0.1 M KOH	36.4	2.8	⁴⁸

Table S5. Comparison of the bifunctional OER and ORR activity of Bi-CoP/NP-DG

with those of the previously reported bifunctional catalysts.

Number	Catalyst	$E_{j10} / V (10 \text{ mA cm}^{-2})$	$E_{1/2} / V$	$\Delta E / V (E_{j10} - E_{1/2})$	Ref
1	Bi-CoP/NP-DG	1.6	0.81	0.79	This work
2	NiCo ₂ S ₄ /N-CNT	1.60	0.80	0.80	⁴⁹
3	CuCo ₂ O ₄ @C	1.62	0.80	0.822	⁵⁰
4	Co@Co ₃ O ₄ /NC-1	1.65	0.80	0.85	⁵¹
5	NiCo/PFC aerogels	1.63	0.77	0.86	⁵²
6	CoO/hi-Mn ₃ O ₄	1.6	0.7	0.9	⁴³
7	NMC/Co@CNTs	1.73	0.79	0.94	⁵³
8	PCN-CFP	1.63	0.67	0.96	⁵⁴
9	NiCo ₂ O ₄ /Graphene	1.67	~0.69	0.98	⁵⁵
10	DN-CP@G	1.788	0.801	0.987	⁵⁶
11	H-Pt/CaMnO ₃	1.80	0.79	1.01	⁵⁷
12	Fe/N-CNT	1.75	0.81	0.94	⁵⁸
13	Co ₃ O ₄ @PGC	1.72	0.69	1.02	⁵⁹
14	Mn oxide	1.77	0.73	1.04	²⁵
15	Co ₃ O ₄ /Co ₂ MnO ₄	1.77	0.68	1.09	⁶⁰

Table S6. Comparison of the power density of Zn-air battery driven by Bi-CoP/NP-

DG with recently reported Zn-air batteries.

Number	Catalyst	Electrolyte	Power density (mW cm ⁻²)	Ref
1	Bi-CoP/NP-DG	6 M KOH + 0.2 M Zn(Ac) ₂	122	This work
2	Co/Co ₃ O ₄ @PGS	6 M KOH + 0.2 M Zn(Ac) ₂	118	²⁶
3	Co ₃ FeS _{1.5} (OH) ₆	6 M KOH + 0.2 M ZnCl ₂	113.1	¹⁰
4	CoNi@NCNT/NF	6 M KOH + 0.2 M Zn(Ac) ₂	108	⁶¹
5	Co/N-CNT	6 M KOH + 0.2 M Zn(Ac) ₂	101	⁶²
6	Co-N,B-CSs	6 M KOH + 0.2 M Zn(Ac) ₂	100.4	²⁰
7	N-GCNT/FeCo-3	6 M KOH + 0.2 M Zn(Ac) ₂	89	²⁴
8	Mn ₃ O ₄ /O-CNT	6 M KOH + 0.2 M ZnCl ₂	86.6	⁵⁶
9	CuCo ₂ O ₄ /N-CNTs	6 M KOH + 0.2 M Zn(Ac) ₂	84	⁶³
10	200-CNTs-Co/NC	6 M KOH + 0.2 M ZnCl ₂	83.1	⁶⁴
11	3DOM Co ₃ O ₄	6 M KOH + 0.2 M Zn(Ac) ₂	80	⁶⁵
12	NiO/CoN PINWs	6 M KOH + 0.2 M Zn(Ac) ₂	79.6	¹⁴
13	Pt/C + Ir/C	6 M KOH + 0.2 M ZnCl ₂	73.4	⁵⁶
14	CoP NCs	3 M KOH + 0.2 M Zn(Ac) ₂	61	⁶⁶
15	CoO NRs	6 M KOH	60.2	⁶⁷

Table S7. Comparison of the performances of Zn-air batteries with various

bifunctional electrocatalysts.

Number	Catalyst	Electrolyte	Specific capacity	Energy density	Cycle Condition	Ref
			(mAh g _{Zn} ⁻¹)	(Wh kg _{Zn} ⁻¹)	(mA cm ⁻²)	
1	Bi-CoP/NP-DG	6 M KOH + 0.2 M Zn(Ac) ₂	752	929	5	This work
2	Mn/Fe-HIB-MOF	6 M KOH + 0.2 M Zn(Ac) ₂	702	788	50	68
3	CuS/NiS ₂ INs	6 M KOH + 0.2 M Zn(Ac) ₂	678	847.5	10	69
4	CoNi@NCNT/NF	6 M KOH + 0.2 M Zn(Ac) ₂	655	845	5	61
5	NiO/CoN PINWs	6 M KOH + 0.2 M Zn(Ac) ₂	648	836	10	14
6	NCNT/CoO-NiO-NiCo	6 M KOH + 0.2 M ZnCl ₂	594	713	7	70
7	NCNF/Co _x Mn _{1-x} O	6 M KOH + 0.2 M ZnCl ₂	581	695	7	71
8	CoZn-NC-700	6 M KOH + 0.2 M ZnCl ₂	578	694	10	16
9	Ag-Cu on Ni foam	6 M KOH + 0.2 M ZnCl ₂	572	641	20	72
10	CoO/N-CNT	6 M KOH + 0.2 M ZnCl ₂	570	700	20	73
11	Co ₃ O ₄ /N-rGO	6 M KOH + 0.2 M ZnCl ₂	550	649	6	3
12	CoO NRs	6 M KOH	541.3	583.3	20	67
13	Ni ₃ Fe/N-C	6 M KOH + 0.2 M ZnCl ₂	528	634	10	35
14	NiCo ₂ S ₄ /N-CNT	6 M KOH + 0.2 M ZnCl ₂	431.1	554.6	10	49
15	ZnCo ₂ O ₄ /N-CNT	6 M KOH	428.47	595.57	10	74

References

- 1 P. Cai, S. Ci, E. Zhang, P. Shao, C. Cao and Z. Wen, *Electrochim. Acta*, 2016, **220**, 354-362.
- 2 M. Shen, C. Ruan, Y. Chen, C. Jiang, K. Ai and L. Lu, *ACS Appl. Mater. Inter.*, 2015, **7**, 1207-1218.
- 3 Y. Li, C. Zhong, J. Liu, X. Zeng, S. Qu, X. Han, Y. Deng, W. Hu and J. Lu, *Adv. Mater.*, 2018, **30**.
- 4 W. Niu, Z. Li, K. Marcus, L. Zhou, Y. Li, R. Ye, K. Liang and Y. Yang, *Adv. Energy. Mater.*, 2018, **8**, 1701642.
- 5 S. Wang, J. Qin, T. Meng and M. Cao, *Nano Energy*, 2017, **39**, 626-638.
- 6 Y. Xu, Y. Hao, G. Zhang, X. Jin, L. Wang, Z. Lu and X. Sun, *Part. Part. Syst. Char.*, 2016, **33**, 569-575.
- 7 A. Kong, Q. Lin, C. Mao, X. Bu and P. Feng, *Chem. Commun.*, 2014, **50**, 15619-15622.
- 8 Y. Su, Y. Zhu, H. Jiang, J. Shen, X. Yang, W. Zou, J. Chen and C. Li, *Nanoscale*, 2014, **6**, 15080-15089.
- 9 J. Wu, S. Dou, A. Shen, X. Wang, Z. Ma, C. Ouyang and S. Wang, *J. Mater. Chem. A*, 2014, **2**, 20990-20995.
- 10 H. F. Wang, C. Tang, B. Wang, B. Q. Li and Q. Zhang, *Adv. Mater.*, 2017, **29**.
- 11 Q. Liu, J. Jin and J. Zhang, *ACS Appl. Mater. Inter.*, 2013, **5**, 5002-5008.
- 12 Y. Chen, X. Jiang, Y. Li, P. Li, Q. Liu, G. Fu, L. Xu, D. Sun and Y. Tang, *Adv. Mater. Interfaces*, 2018, **5**, 1701015.
- 13 Z. Zhang, X. Wang, G. Cui, A. Zhang, X. Zhou, H. Xu and L. Gu, *Nanoscale*, 2014, **6**, 3540-3544.
- 14 J. Yin, Y. Li, F. Lv, Q. Fan, Y. Q. Zhao, Q. Zhang, W. Wang, F. Cheng, P. Xi and S. Guo, *ACS nano*, 2017, **11**, 2275-2283.
- 15 X. Zhang, R. Liu, Y. Zang, G. Liu, G. Wang, Y. Zhang, H. Zhang and H. Zhao, *Chem. Commun.*, 2016, **52**, 5946-5949.
- 16 B. Chen, X. He, F. Yin, H. Wang, D.-J. Liu, R. Shi, J. Chen and H. Yin, *Adv. Funct. Mater.*, 2017, **27**, 1700795.
- 17 L. Ma, S. Chen, Z. Pei, Y. Huang, G. Liang, F. Mo, Q. Yang, J. Su, Y. Gao, J. A.

- Zapien and C. Zhi, *ACS nano*, 2018, **12**, 1949-1958.
- 18 S. Liu, Z. Wang, S. Zhou, F. Yu, M. Yu, C. Y. Chiang, W. Zhou, J. Zhao and J. Qiu, *Adv. Mater.*, 2017, **29**.
- 19 Z. Wen, S. Ci, Y. Hou and J. Chen, *Angew. Chem. Int. Ed.*, 2014, **53**, 6496-6500.
- 20 Y. Guo, P. Yuan, J. Zhang, Y. Hu, I. S. Amiinu, X. Wang, J. Zhou, H. Xia, Z. Song, Q. Xu and S. Mu, *ACS nano*, 2018, **12**, 1894-1901.
- 21 Q. Wang, Y. Ji, Y. Lei, Y. Wang, Y. Wang, Y. Li and S. Wang, *ACS Energy Lett.*, 2018, **3**, 1183-1191.
- 22 Z. Pei, H. Li, Y. Huang, Q. Xue, Y. Huang, M. Zhu, Z. Wang and C. Zhi, *Energ. Environ. Sci.*, 2017, **10**, 742-749.
- 23 J. Wang, H. Wu, D. Gao, S. Miao, G. Wang and X. Bao, *Nano Energy*, 2015, **13**, 387-396.
- 24 C.-Y. Su, H. Cheng, W. Li, Z.-Q. Liu, N. Li, Z. Hou, F.-Q. Bai, H.-X. Zhang and T.-Y. Ma, *Adv. Energy Mater.*, 2017, **7**, 1602420.
- 25 W. Zhang, Y. Hu, L. Ma, G. Zhu, P. Zhao, X. Xue, R. Chen, S. Yang, J. Ma, J. Liu and Z. Jin, *Nano Energy*, 2018, **53**, 808-816.
- 26 Y. Fu, H.-Y. Yu, C. Jiang, T.-H. Zhang, R. Zhan, X. Li, J.-F. Li, J.-H. Tian and R. Yang, *Adv. Funct. Mater.*, 2018, **28**, 1705094.
- 27 C. Zhang, G. Zhang, H. Li, Y. Chang, Z. Chang, J. Liu and X. Sun, *Electrochim. Acta*, 2017, **247**, 1044-1051.
- 28 Q. Liu, Y. Wang, L. Dai and J. Yao, *Adv. Mater.*, 2016, **28**, 3000-3006.
- 29 W. Yang, G. Chata, Y. Zhang, Y. Peng, J. E. Lu, N. Wang, R. Mercado, J. Li and S. Chen, *Nano Energy*, 2019, **57**, 811-819.
- 30 L. Zhu, D. Zheng, Z. Wang, X. Zheng, P. Fang, J. Zhu, M. Yu, Y. Tong and X. Lu, *Adv. Mater.*, 2018, **30**, e1805268.
- 31 Z. Wu, J. Wang, M. Song, G. Zhao, Y. Zhu, G. Fu and X. Liu, *ACS Appl. Mater. Interfaces*, 2018, **10**, 25415-25421.
- 32 R. Zhang, L. Wang, Y.-H. Ma, L. Pan, R. Gao, K. Li, X. Zhang and J.-J. Zou, *J. Mater. Chem. A*, 2019, **7**, 10010-10018.
- 33 R. K. Bera, H. Park and R. Ryoo, *J. Mater. Chem. A*, 2019, **7**, 9988-9996.

- 34 H. Jiang, J. Gu, X. Zheng, M. Liu, X. Qiu, L. Wang, W. Li, Z. Chen, X. Ji and J. Li, *Energy Environ. Sci.*, 2019, **12**, 322-333.
- 35 G. Fu, Z. Cui, Y. Chen, Y. Li, Y. Tang and J. B. Goodenough, *Adv. Energy Mater.*, 2017, **7**, 1601172.
- 36 G. Fu, X. Jiang, Y. Chen, L. Xu, D. Sun, J.-M. Lee and Y. Tang, *NPG Asia Mater.*, 2018, **10**, 618-629.
- 37 G. Fu, Z. Liu, J. Zhang, J. Wu, L. Xu, D. Sun, J. Zhang, Y. Tang and P. Chen, *Nano Res.*, 2016, **9**, 2110-2122.
- 38 Z. Pei, H. Li, Y. Huang, Q. Xue, Y. Huang, M. Zhu, Z. Wang and C. Zhi, *Energy Environ. Sci.*, 2017, **10**, 742-749.
- 39 G. Li, L. Pei, Y. Wu, B. Zhu, Q. Hu, H. Yang, Q. Zhang, J. Liu and C. He, *J. Mater. Chem. A*, 2019, **7**, 11223-11233.
- 40 Y.-N. Chen, Y. Guo, H. Cui, Z. Xie, X. Zhang, J. Wei and Z. Zhou, *J. Mater. Chem. A*, 2018, **6**, 9716-9722.
- 41 H. Fang, T. Huang, D. Liang, M. Qiu, Y. Sun, S. Yao, J. Yu, M. M. Dinesh, Z. Guo, Y. Xia and S. Mao, *J. Mater. Chem. A*, 2019, **7**, 7328-7332.
- 42 G. Fu, J. Wang, Y. Chen, Y. Liu, Y. Tang, J. B. Goodenough and J.-M. Lee, *Adv. Energy Mater.*, 2018, **8**, 1802263.
- 43 C. Guo, Y. Zheng, J. Ran, F. Xie, M. Jaroniec and S. Z. Qiao, *Angew. Chem. Int. Ed.*, 2017, **56**, 8539-8543.
- 44 G. Fu, Z. Cui, Y. Chen, L. Xu, Y. Tang and J. B. Goodenough, *Nano Energy*, 2017, **39**, 77-85.
- 45 A. Ashok, A. Kumar, J. Ponraj, S. A. Mansour and F. Tarlochan, *Int. J. Hydrogen Energ.*, 2019, **44**, 16603-16614.
- 46 X. Hu, T. Huang, Y. Tang, G. Fu and J. M. Lee, *ACS Appl. Mater. Interfaces*, 2019, **11**, 4028-4036.
- 47 G. Fu, Y. Wang, Y. Tang, K. Zhou, J. B. Goodenough and J.-M. Lee, *ACS Materials Lett.*, 2019, **1**, 123-131.
- 48 G. Fu, Y. Liu, Y. Chen, Y. Tang, J. B. Goodenough and J. M. Lee, *Nanoscale*, 2018, **10**, 19937-19944.

- 49 S. Hu, T. Han, C. Lin, W. Xiang, Y. Zhao, P. Gao, F. Du, X. Li and Y. Sun, *Adv. Funct. Mater.*, 2017, **27**, 1700041.
- 50 W. Jin, J. Chen, Z. Wu and G. Maduraiveeran, *Int. J. Hydrogen Energ.*, 2019, **44**, 11421-11430.
- 51 A. Aijaz, J. Masa, C. Rosler, W. Xia, P. Weide, A. J. Botz, R. A. Fischer, W. Schuhmann and M. Muhler, *Angew. Chem. Int. Ed.*, 2016, **55**, 4087-4091.
- 52 G. Fu, Y. Chen, Z. Cui, Y. Li, W. Zhou, S. Xin, Y. Tang and J. B. Goodenough, *Nano Lett.*, 2016, **16**, 6516-6522.
- 53 S. Cai, R. Wang, W. Guo and H. Tang, *Langmuir : the ACS journal of surfaces and colloids*, 2018, **34**, 1992-1998.
- 54 T. Y. Ma, J. Ran, S. Dai, M. Jaroniec and S. Z. Qiao, *Angew. Chem. Int. Ed.*, 2015, **54**, 4646-4650.
- 55 D. U. Lee, B. J. Kim and Z. Chen, *J. Mater. Chem. A*, 2013, **1**, 4754.
- 56 C. Hang, J. Zhang, J. Zhu, W. Li, Z. Kou and Y. Huang, *Adv. Energy Mater.*, 2018, **8**, 1703539.
- 57 X. Han, F. Cheng, T. Zhang, J. Yang, Y. Hu and J. Chen, *Adv. Mater.*, 2014, **26**, 2047-2051.
- 58 Y. Liu, H. Jiang, Y. Zhu, X. Yang and C. Li, *J. Mater. Chem. A*, 2016, **4**, 1694-1701.
- 59 G. Li, X. Wang, J. Fu, J. Li, M. G. Park, Y. Zhang, G. Lui and Z. Chen, *Angew. Chem. Int. Ed.*, 2016, **55**, 4977-4982.
- 60 D. Wang, X. Chen, D. G. Evans and W. Yang, *Nanoscale*, 2013, **5**, 5312-5315.
- 61 W. Niu, S. Pakhira, K. Marcus, Z. Li, J. L. Mendoza-Cortes and Y. Yang, *Adv. Energy Mater.*, 2018, **8**, 1800480.
- 62 T. Wang, Z. Kou, S. Mu, J. Liu, D. He, I. S. Amiinu, W. Meng, K. Zhou, Z. Luo, S. Chaemchuen and F. Verpoort, *Adv. Funct. Mater.*, 2018, **28**, 1705048.
- 63 H. Cheng, M.-L. Li, C.-Y. Su, N. Li and Z.-Q. Liu, *Adv. Funct. Mater.*, 2017, **27**, 1701833.
- 64 S. Liu, I. S. Amiinu, X. Liu, J. Zhang, M. Bao, T. Meng and S. Mu, *Chem. Eng. J.*, 2018, **342**, 163-170.

- 65 M. G. Park, D. U. Lee, M. H. Seo, Z. P. Cano and Z. Chen, *Small*, 2016, **12**, 2707–2714.
- 66 H. Li, Q. Li, P. Wen, T. B. Williams, S. Adhikari, C. Dun, C. Lu, D. Itanze, L. Jiang, D. L. Carroll, G. L. Donati, P. M. Lundin, Y. Qiu and S. M. Geyer, *Adv. Mater.*, 2018, **30**.
- 67 P. Da, M. Wu, K. Qiu, D. Yan, Y. Li, J. Mao, C. Dong, T. Ling and S. Qiao, *Chem. Eng. Sci.*, 2019, **194**, 127-133.
- 68 S. S. Shinde, C. H. Lee, J.-Y. Jung, N. K. Wagh, S.-H. Kim, D.-H. Kim, C. Lin, S. U. Lee and J.-H. Lee, *Energ. Environ. Sci.*, 2019, **12**, 727-738.
- 69 L. An, Y. Li, M. Luo, J. Yin, Y.-Q. Zhao, C. Xu, F. Cheng, Y. Yang, P. Xi and S. Guo, *Adv. Funct. Mater.*, 2017, **27**, 1703779.
- 70 X. Liu, M. Park, M. G. Kim, S. Gupta, G. Wu and J. Cho, *Angew. Chem. Int. Ed.*, 2015, **54**, 9654-9658.
- 71 X. Liu, M. Park, M. G. Kim, S. Gupta, X. Wang, G. Wu and J. Cho, *Nano Energy*, 2016, **20**, 315-325.
- 72 Y. Jin and F. Chen, *Electrochim. Acta*, 2015, **158**, 437-445.
- 73 Y. Li, M. Gong, Y. Liang, J. Feng, J. E. Kim, H. Wang, G. Hong, B. Zhang and H. Dai, *Nat. Commun.*, 2013, **4**, 1805.
- 74 Z. Q. Liu, H. Cheng, N. Li, T. Y. Ma and Y. Z. Su, *Adv. Mater.*, 2016, **28**, 3777-3784.